Molecular Microbiology (2011) 79(4), 1101–1117 ■

doi:10.1111/j.1365-2958.2010.07511.x
First published online 5 January 2011

Evidence for branching in cryptococcal capsular polysaccharides and consequences on its biological activity

Radames J. B. Cordero,[1†] Susana Frases,[1,3†] Allan J. Guimaräes,[1,2] Johanna Rivera[1] and Arturo Casadevall[1,2*]

Departments of [1]Microbiology and Immunology and [2]Medicine (Division of Infectious Diseases), Albert Einstein College of Medicine of Yeshiva University, Bronx, NY, USA.

[3]Laboratório de Biotecnologia – LABIO, Instituto Nacional de Metrologia, Normalização e Qualidade Industrial – INMETRO, Av. Nossa Senhora das Graças, 50 – Xerém, Rio de Janeiro, Brazil, CEP: 25 250 020.

Summary

The encapsulated fungus *Cryptococcus neoformans* is a common cause of life-threatening disease in immunocompromised individuals. Its major virulence determinant is the polysaccharide (PS) capsule. An unsolved problem in cryptococcal biology is whether the PSs composing the capsule are linear or complex branched polymers, as well as the implications of this structural composition in pathogenesis. In this study we approached the problem by combining static and dynamic light scattering, viscosity analysis, and high-resolution microscopy and correlated the findings with biological properties. Analysis of the dependence of capsular PS molecular mass and the radius of gyration provided strong evidence against a simple linear PS configuration. Shape factors calculated from light scattering measurements in solution revealed values consistent with polymer branching. Furthermore, viscosity measurements provided complementary evidence for structural branching. Electron microscopy showed PS spherical-like structures similar to other branched PS. Finally, we show that the capacity of capsular PS to interfere in complement-mediated phagocytosis, inhibit nitric oxide production by macrophage-like cells, protect against reactive oxygen species, antibody reactivity and half-life in serum were influenced by the degree of branching, providing evidence for the notion that PS branching is an important parameter in determining the biological activity of *C. neoformans* PS.

Accepted 9 December, 2010. *For correspondence. E-mail casadeva@aecom.yu.edu; Tel. (718) 430-2215; Fax (718) 430 8968. The data in this paper are from a thesis to be submitted by Radames J.B. Cordero in partial fulfilment of the requirements for Doctor of Philosophy degree in the Sue Golding Graduate Division of Medical Science, Albert Einstein College of Medicine, Yeshiva University, Bronx, NY, USA. †RJBC and SF contributed equally to this work.

Introduction

Cryptococcus neoformans is an encapsulated fungus that is responsible for cryptococcosis, a life-threatening disease with a worldwide distribution that particularly affects individuals with impaired immunity. Recent epidemiological studies indicate that cryptococcosis has eclipsed tuberculosis as a cause of death in Sub-Saharan Africa (Park *et al.*, 2009). The major virulence factor of this pathogen is a PS capsule surrounding the cell body (Chang and Kwon-Chung, 1994; McClelland *et al.*, 2005). The capsule is believed to contribute to virulence by protecting the fungal cells against host immunity. During infection and pathogen–host interactions, cryptococcal PS is shed or secreted into the external milieu resulting in deleterious immunological effects such as antibody unresponsiveness (Murphy and Cozad, 1972; Kozel *et al.*, 1977), inhibition of leukocyte migration (Dong and Murphy, 1995), depletion of complement (Macher *et al.*, 1978), cytokine production (Vecchiarelli *et al.*, 1995; Retini *et al.*, 1996), interference with antigen presentation (Retini *et al.*, 1998) and prevention of phagocytosis by macrophages (Kozel and Gotschlich, 1982). Changes in capsular antigenic structure and size have been described and associated with brain invasion (Charlier *et al.*, 2005), correlating structural variability with cryptococcal crossing of the blood–brain barrier. The capsule is also the target for experimental PS conjugate vaccines and passive antibody therapies (Pirofski, 2001; Larsen *et al.*, 2005).

Despite the importance of the *C. neoformans* capsule in virulence, little is known about the physical and biochemical characteristics of the PSs that are responsible for the capsule structure and its many biological effects. The capsule is complex and composed of at least two major PSs, glucuronoxylomannan (GXM) and glucuronoxylomannogalactan (GXMGal) (Cherniak and Sundstrom, 1994; Doering, 2000; Grijpstra *et al.*, 2009; Heiss *et al.*, 2009;

Zaragoza *et al*., 2009). GXM polymers comprise more than 90% of the total capsular mass, and are characterized by large molecular masses (1700–7000 kDa) (McFadden *et al*., 2006b). GXM consists of an α-(1,3)-mannan main chain with β(1,2)-glucuronic acid residues attached to every third mannose, on average. Mannosyl residues can also be 6-*O*-acetylated and substituted with xylosyl units in β(1,2)- or β(1,4)-linkages (Cherniak *et al*., 1998). GXMGal consists of a α-(1,6) galactan backbone with side-chain substitutions of mannose, xylose and glucuronic acid residues. Xylose molecules can also be associated to mannose rings through β(1,3) or β(1,2) linkages (Vaishnav *et al*., 1998).

While bacterial PSs have single oligosaccharide-repeating units, GXM has at least seven different structural reporter groups or motifs (Bacon *et al*., 1996; Cherniak *et al*., 1998; Nimrichter *et al*., 2007), identified by ^{1}H-NMR based on the shift of the anomeric protons and mannosyl residues (Cherniak *et al*., 1998). Moreover, mass spectroscopy of fragmented molecules suggested that certain GXM are heterodimers composed of different GXM structural reporter group repeating units (McFadden *et al*., 2007). Adding to this diversity was the observation that those strains differed in serotypes by the ratio of those units within the GXM molecule and by the extent of mannose *O*-acetylation (Cherniak and Sundstrom, 1994; McFadden *et al*., 2007). This observation raised the possibility of almost unlimited diversity in PS molecule primary, secondary and tertiary structures that can translate into antigenic and physico-chemical variability. The existence of secondary and tertiary PS structures is indeed expected, as a result of the enormous potential of GXM to form inter- and intra-molecular hydrogen bonds and the well-known ability of eukaryotic glycosyltransferases to catalyse the formation of branched structures (Stoddart, 1984).

An assumption in the cryptoccocal field is that the capsular PSs are simple linear polymer structures, with the caveat that this supposition is based largely on the absence of data for branching rather than on direct evidence for linearity (Doering, 2009). In this study, we revisit the problem of cryptococcal capsular PS structure by taking a physical–chemical approach that combined static and dynamic light scattering (SLS and DLS, respectively) with viscosity studies, and complemented with high-resolution microscopy. The strategy was to derive inferences about capsular PS structure from measured average-molecular mass (M_w), mean-square radius of gyration (R_g), hydrodynamic radius (R_h), viscosity and other physical parameters. Our studies provide compelling evidence that cryptococcal capsular PS molecules are large, structurally compacted and branched, resulting in highly complex polymer structures. Furthermore, analyses of the biological activity of capsular PS strongly suggest that the degree of branching and conformation are important parameters in determining the biological activity of *C. neoformans* PS.

Results

Biophysical evidence for branched structures

We sought to obtain evidence for PS branching by applying polymer solution theory using information from light scattering (LS) techniques. Consequently, we compiled this information from a set of capsular PS samples systematically isolated from seven different cryptococcal strains (representing all five serotypes A, D, B, C and AD) grown and treated under equal conditions. In addition, as a control for our measurements, we tested different capsular PS extraction methods and studied four well-characterized non-cryptococcal and glucose-composed PSs that are known to differ in structure and M_w. These controls were two branched (amylopectin and glycogen) and two linear (amylose and pullulan) PSs. Analysis of PS samples were done without size fractionation; thus, the interpretation of data was based on the average values measured by both DLS and SLS techniques. Determination of the power law behaviour between M_w and R_g, shape factor and viscosity provided results consistent with polymer branching and high structure complexity.

First, the dependence of molecular parameters on salt concentration was tested with capsular PS isolated from *C. neoformans* H99 cells and suspended in aqueous solutions with different NaCl concentration (0.1, 10 and 100 mM). Under these conditions, almost identical values of M_w and R_g were obtained with 10 and 100 mM NaCl and consequently all experiments in this study were performed using 10 mM NaCl. Recent studies revealed that divalent cations can form bridges across glucuronic acid residues (Nimrichter *et al*., 2007), resulting in non-covalent cross-links of PS molecules. Because this phenomenon could overestimate the LS-derived molecular parameters, we carried out measurements of isolated capsular PS before and after chelation by EDTA. Berry plots obtained from SLS data for all the cryptococcal strains showed an angular dependence and linear concentration dependence, regardless of EDTA treatment (See Fig. S1 for example of a representative Berry plot). The M_w of capsular PS samples isolated from the different cryptococcal strains ranged from 10^7–10^8 g mol^{-1}, indicating that PS mass can vary substantially (up to 10-fold) between strains (Table S1). In addition, the M_w of capsular PSs were shifted to lower values upon EDTA treatment, consistent with the influence of divalent cations on PS aggregation and the consequent additive effects on the molecular mass of GXM. Corresponding changes in the R_g were also observed depending on EDTA treatment, with values ranging from 158 to 239 nm in size. However,

no significant variation in M_w and R_g was observed for the MAS92-203 strain. The R_h values decreased upon EDTA treatment for most of the samples with the exception of the PS isolated from the NIH 444 strain. Relative to the R_g, the R_h values ranged from 570 to 2434 nm, indicating a variation of up to ~4-fold in hydrodynamic size. Polydispersity values were comparable for all capsular PS samples ($P > 0.1$), regardless of EDTA treatment. These results were in agreement with a great structural diversity in PS samples from strains in the *Cryptococcus* complex.

There were differences in the LS-derived parameters for PS samples isolated using different methods, confirming previous studies (Frases *et al*., 2008). The largest values of M_w were obtained for the DMSO-extracted PS sample (DMSO-PS), while the lowest were obtained for both F- and GR-PS samples (PS isolated by ultrafiltration and gamma-radiation, respectively). Whereas, the PS sample isolated by cetyltrimethylammonium bromide precipitation (CTAB-PS) showed the second largest M_w value, it also exhibited the smallest R_g. Hydrodynamic sizes (R_h) varied in a manner similar to the M_w. PS isolated by DMSO and gamma-radiation yielded the highest and the lowest R_h value respectively. Polydispersity values showed differences depending on the isolation method used, the largest and the lowest values (which fall out of the standard deviation limits) were obtained for CTAB-PS and GR-PS respectively. As a control for our methodology, we measured the same molecular parameters for several well-characterized PS (Table S1) and our values are in accord with published reports (Nordmeier, 1993; Bello-Pérez *et al*., 1998; Millard *et al*., 1999; Roger *et al*., 2000; Radosta *et al*., 2001; Rolland-Sabate *et al*., 2007; Morris *et al*., 2008).

M_w *and size dependence.* The relationship between macro-structural parameters such as the M_w, and R_g obtained by SLS and DLS was examined (Fig. 1A). This relationship is described by the power law, $R_g = KM_w^v$ (Hanselmann *et al*., 1996). The scaling exponent, v, obtained from the power fit of a double logarithmic plot, can provide direct evidence for polymer branching, as linear and branched polymers yield differences in the change of molecular size as a function of molecular mass (Burchard *et al*., 1980). Power fits from the M_w and R_g of capsular PS samples and four well-characterized PS are shown in Fig. 1A. The v for the M_w dependence of R_g for capsular PS isolated from all seven cryptococcal strains (with and without EDTA treatment) was ~0.2. In contrast to values from linear PSs such as pullulan (~0.6) (Nordmeier, 1993; Roger *et al*., 2000) and amylose (~0.5) (Roger *et al*., 2000), cryptococcal capsular PSs gave values close to the ones observed for the branched PSs amylopectin (~0.3) (Bello-Pérez *et al*., 1998; Rolland-Sabate *et al*., 2007) and glycogen (~0.3) (Morris *et al*., 2008).

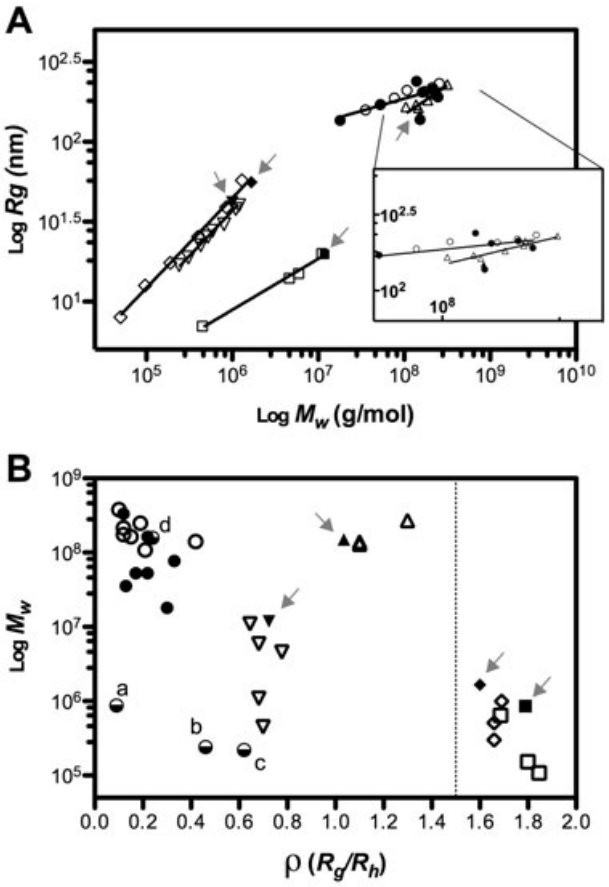

Fig. 1. (A) The M_w dependence of R_g of cryptococcal capsular PS samples; before (○) and after (●) divalent cation chelation with EDTA. Each point (○,●) represents the data of capsular PS from a different *C. neoformans* strain isolated by DMSO extraction (See Table S1 for data values). Data points for standard PSs [amylopectin (△), glycogen (▽), pullulan (◇) and amylose (□)] were taken from (Roger *et al*., 2000; Rolland-Sabate *et al*., 2007; Morris *et al*., 2008) (See Table S3 for data values). Filled symbols and arrows indicate the values obtained with our conditions for each of these four standard PSs. (B) The shape factor (ρ) parameter. Data are displayed using plotting symbols as in A. The ρ of cryptococcal PS isolated by different methods (half-filled circles)) are labelled as a, b, c and d, for CTAB-, F-, GR- and DMSO-PS, respectively. Data points for standard PSs were taken from (Nordmeier, 1993; Bello-Pérez *et al*., 1998; Radosta *et al*., 2001; Morris *et al*., 2008) (See Table S3 for data values). Vertical dashed line in (B) represents the cut-off point (1.5) for the determination of branched molecules. Values lower than 1.5 represent branched and higher, linear polymers.

The shape factor (ρ) *parameter.* The ρ of a polymer is determined by the ratio of R_g to R_h and provides an important insight into whether a molecule is a loosely linear or a branched compacted structure (Nilsson *et al*., 2006; Murakami *et al*., 2008). This dimensionless quantity provides information of molecular conformation and is a function of the branching density, polydispersity and flexibility of the PS subchains and does not depend on the bond length or the degree of polymerization (Burchard *et al*., 1980). Shape factors calculated for capsular PSs isolated

from all cryptococcal strains ranged from 0.1 to 0.4 (Fig. 1B). These values were much lower than for linear flexible polymers (which range from 1.5–1.7), theoretical values for monodispersed hard spheres 0.775 (Burchard and Patterson, 1983), or even values characteristic of hyperbranched structures such as amylopectin (~1.0) (Millard *et al.*, 1999) and glycogen (~0.7) (Morris *et al.*, 2008). This result strongly argues against a linear conformation and implies a high degree of polymer branching and/or compacted conformation in aqueous solution. In all cases, a slight increment in ρ was observed after chelation of divalent cations, consistent with disruption of aggregation and/or some compaction release by ion-mediated intramolecular cross-links. Values obtained for amylopectin, glycogen, pullulan and amylose were in agreement with published results (Nordmeier, 1993; Bello-Pérez *et al.*, 1998; Millard *et al.*, 1999; Roger *et al.*, 2000; Radosta *et al.*, 2001; Rolland-Sabate *et al.*, 2007; Morris *et al.*, 2008).

Shape factor values varied depending on the method of extraction (Fig. 1B). The largest and lowest ρ values were obtained for the GR-PS and CTAB-PS samples, respectively. Under our conditions, no significant correlation was detected between the capsule size and ρ values obtained from the different cryptococcal strains (Fig. S2).

Electron microscopy revealed branched-like PS structures. Capsular PS isolated from *C. neoformans* H99 cell culture grown in minimal media was examined by transmission electron microscopy (TEM) after negative staining. Branched rosette-like structures were observed (Fig. 2A) that were similar to those described for glycogen, a hyperbranched PS (Childress *et al.*, 1970). From these images, we were able to measure an apparent diameter for capsular PS (Fig. 2B). This diameter measured by microscopy was similar to that calculated from DLS (inset Fig. 2B), providing a reassuring concordance between microscopic and solution physical–chemical measurements. The discrepancies in diameter values obtained from both techniques were expected, as DLS measures hydrodynamic sizes of polymers in solution and the method tends to overestimate diameter as larger molecules scatter disproportionately more (Davis *et al.*, 1994; Eisenman *et al.*, 2009).

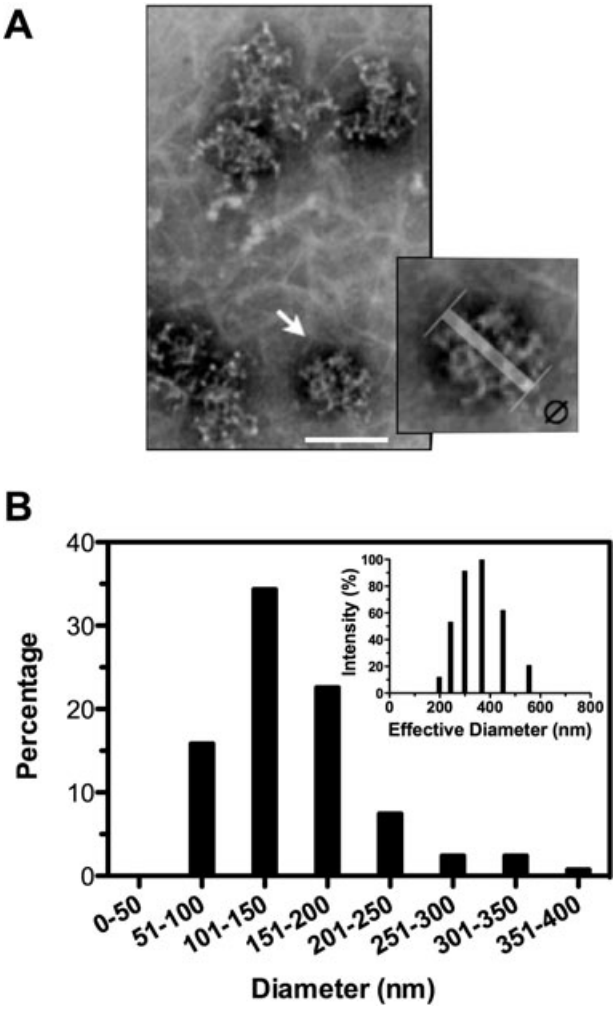

Fig. 2. Electron microscopic evidence for branched structures in *C. neoformans* capsular PS.
A. TEM images of negatively stained extracted capsular PS from *C. neoformans* H99 cells. Scale bar represents 200 μm. Inset shows an enlarged section of PS polymers resembling a rosette-like structure.
B. Size distribution of measured diameters (Ø) of hyperbranched structures expressed as percentage. Inset shows multimodal hydrodynamic size distribution of PS samples determined by DLS.

Biological effects of capsule PS branching

To examine the potential biological effects of capsular PS branched structures, we needed conditions where we could induce variations in the branching degree while retaining comparable monosaccharide compositions. We focused on the H99 strain and approached the problem by varying growth conditions that affect the capsule, such as the concentration of dextrose, which can also affect PS structure as inferred by differences in R_h (Cleare and Casadevall, 1999; Guimaraes *et al.*, 2010). Consequently, *C. neoformans* H99 cells were cultured in minimal media supplemented with 15 (regular), 62.5, 125, 250 and 500 mM of dextrose. Cells were washed with phosphate buffer saline (PBS) solution and analysed by light microscopy after India-ink staining and scanning electron microscopy (Fig. 3A). Consistent with capsular repression by dextrose (Dykstra *et al.*, 1977), our results showed a trend towards smaller capsules with higher dextrose concentrations ($r = -0.86$) (Fig. 3B), as reported previously (Guimaraes *et al.*, 2010). SEM micrographs of whole cells

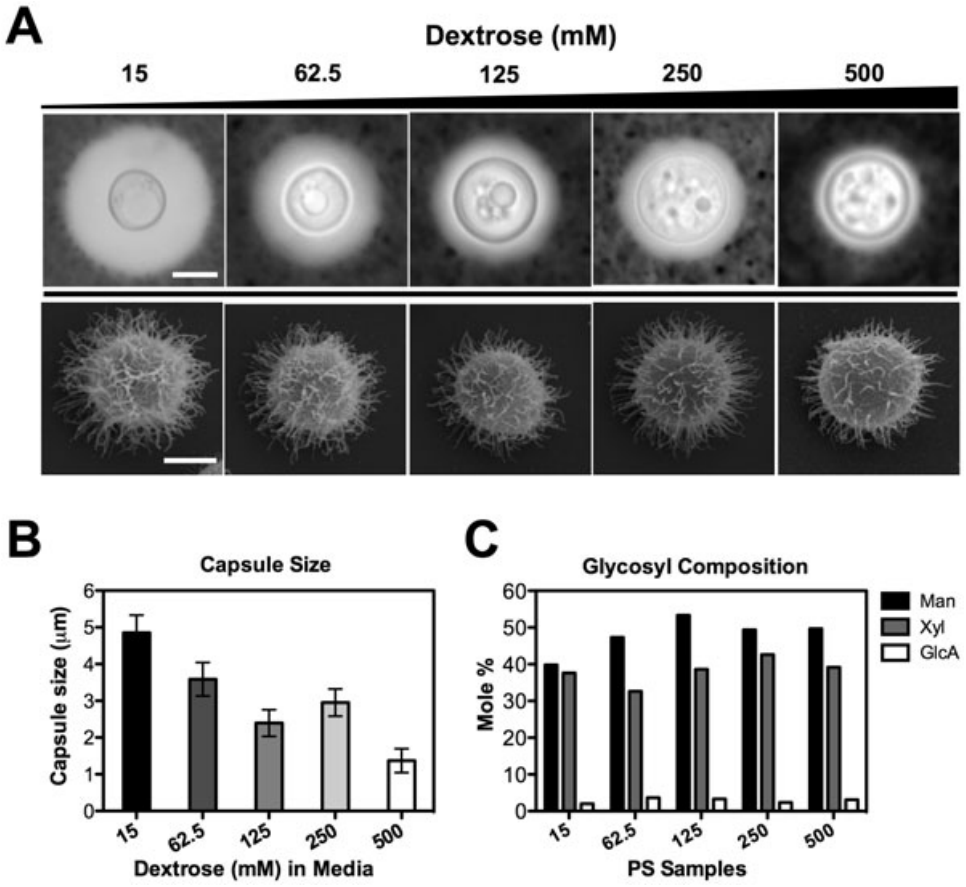

Fig. 3. The relationship of capsule size and glycosyl composition of H99 cells as a function of dextrose concentration.
A. Micrographs of the different H99 cultures in suspension visualized by India-ink staining and SEM (scale bar represents 5 and 2 μm, respectively).
B Capsule size measurements of cells grown in different dextrose concentrations. Data are represented as mean ± standard deviation (SD).
C. Glycosyl composition analysis of the DMSO-extracted capsular PS samples. Data are represented as mole percentage of mannose (Man), xylose (Xyl) and glucuronic acid (GlcA).

revealed tangled fibrillar structures on the cell surface suggestive of PS collapse as a result of dehydration (Cleare and Casadevall, 1999). Nevertheless, the apparent capsule observed from SEM images correlated with the decrease in capsule size determined by light microscopy.

The glycosyl composition analysis revealed that the molar percentage of mannose, xylose and glucuronic acid between the different PS samples were similar, indicating that the GXM PS chemical composition did not significantly vary ($P > 0.05$) as a function of dextrose concentration (Fig. 3C). This result is in agreement with several studies, showing that sugar composition of capsular PS is relatively invariant (McFadden *et al.*, 2007; Frases *et al.*, 2008; 2009). However, the R_h and M_w of capsular PSs tended to decrease with increasing dextrose concentration ($r = -0.80$) (Table S2). Shape factors tended to vary in a dextrose dependent manner ($r = 0.83$), consistent with different degrees of polymer branching, compaction and/or complexity; the smallest and largest ρ were found to be associated with the lowest and highest dextrose concentrations respectively (Table S2).

The distinct degrees of polymer branching obtained for this set of capsular PS samples were confirmed by means of their viscosity measurements. First, rheological behaviour of capsular PS solutions at different concentrations isolated from H99 cells grown in minimal media was examined by a stress-controlled steady shear measurement. Solutions of PS with concentrations ranging from 0.1 to 0.025 mg ml^{-1} showed simple Newtonian behaviour with viscosity values in the range of 1–2 centipoise (Fig. 4A and inset). As expected, the viscosity increased with increasing PS concentration. However, solutions containing 1.0 mg ml^{-1} of capsular PS exhibited shear-thinning (i.e. a decrease in viscosity when the shear gradient is increased), which is a behaviour typical of an entangled polymer solution (Ferry, 1980). In contrast, pullulan and amylopectin solutions exhibited Newtonian flow

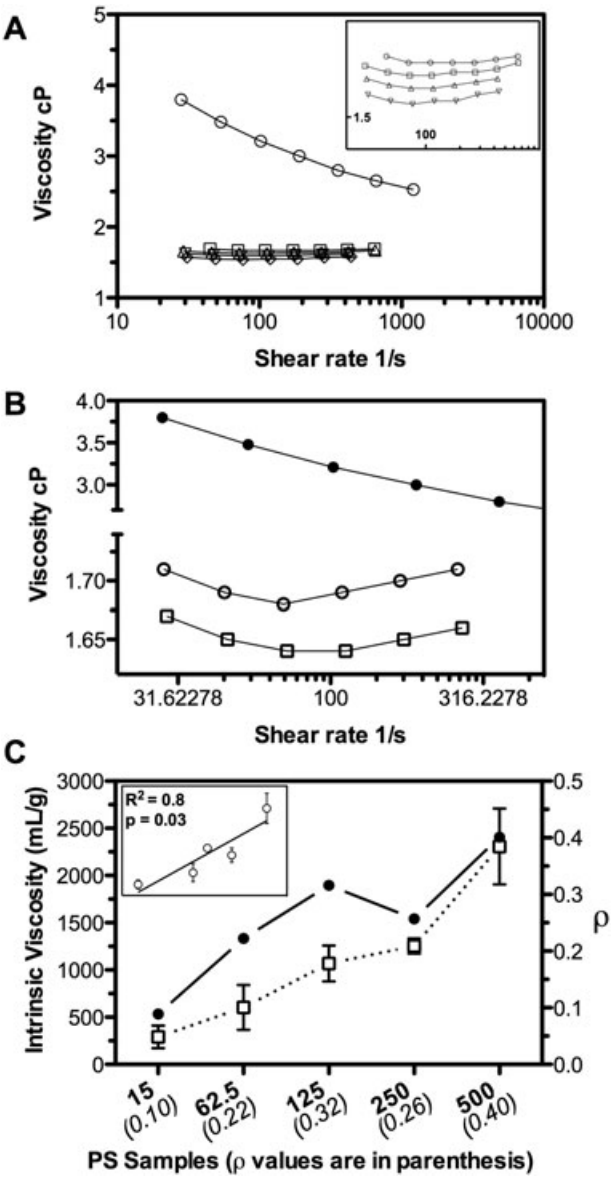

Fig. 4. Viscosity of *C. neoformans* capsular PS.
A. Steady shear viscosity of H99 capsular PS at different PS concentrations: 1.0 (○), 0.1 (□), 0.075 (△), 0.05 (▽), 0.025 (◇) mg ml^{-1}.
B. Steady shear viscosity of H99 capsular PS (●), pullulan (○) and amylopectin (□) at 1 mg ml^{-1}.
C. Correlation between intrinsic viscosity (□) and ρ (●) of PS samples DMSO-extracted from H99 cells grown at different dextrose concentrations. Insert plot depicts the linear regression analysis between intrinsic viscosity versus ρ. Error bars represent SD.

(Fig. 4B). Intrinsic viscosity measurements of capsular PS samples isolated from cultures supplemented with different dextrose concentrations were performed using the range of PS concentration where Newtonian behaviour was observed. Differences in intrinsic viscosity were detected depending on the dextrose concentration ($r = 0.98$, $P < 0.003$) (Fig. 4C). These values were, in turn, directly proportional to the ρ ($R^2 = 0.83$, $P = 0.03$) of PS molecules (Fig. 4C), confirming an association between ρ and viscosity.

Effect of capsular PS branching in complement-mediated phagocytosis. Given that H99 cells grown in different concentrations of dextrose produced capsular PS with different degrees of PS branching as inferred by analysis of their ρ and intrinsic viscosity, we investigated the effect of branching on phagocytic efficacy using complement as opsonin. The efficiency of complement-mediated phagocytosis decreased for cells grown with increasing dextrose concentrations (Fig. 5A), which expressed less branched PS (higher ρ), suggesting a possible correlation between capsule PS structure and phagocytosis ($r = -0.9$, $P = 0.08$) (Fig. 5B). In contrast, a positive trend was observed between capsule size and efficiency of phagocytosis of H99 cells ($r = 0.9$, $P = 0.08$) (Fig. 5C), where cells with smaller capsules were phagocytosed less. No trend was observed when the glycosyl composition was analysed against the percentage of phagocytosis [Mannose; ($r = -0.7$, $P = 0.23$), Xylose; ($r = -0.8$, $P = 0.13$), Glucuronic Acid; ($r = -0.1$, $P = 0.95$)] (Fig. 5D). This was expected as no significant variations in glycosyl composition were detected between these growth conditions (Fig. 3C). Given that both ρ and capsule size were altered when cells were grown in different amounts of dextrose, and that neither variable had a significant correlation with phagocytosis at the 0.05 level, we found it difficult to conclusively assess the effect of PS branching on phagocytosis using whole cells. Consequently, we investigated the effect of branching on phagocytic efficacy by measuring the ability of isolated soluble capsular PS to inhibit phagocytosis of complement-opsonized yeast cells. This approach was suggested by the observation that soluble PS can inhibit phagocytosis (Kozel and Mastroianni, 1976) and we hypothesized that capsular PS isolated from cells grown in different dextrose concentrations, and exhibiting distinct degrees of branching and complexity, would vary in its ability to interfere with this process. The percentage of phagocytosis decreased in the presence of capsular PS (Fig. 6A). Distinct inhibitory capacities were evident for PS extracted from cells grown in different dextrose concentrations (Fig. 6A). The highest inhibition was observed for PS obtained from cultures with the highest dextrose concentration, which corresponded to the less branched PS (higher ρ). The efficacy of complement-mediated phagocytosis was inversely proportional to the ρ ($r = -1.0$, $P = 0.02$) (Fig. 6B). These results show that the ability of capsular PS to interfere with the efficiency of complement-mediated phagocytosis can be modulated by polymer structure, and less branched PSs are able to inhibit this process more efficiently.

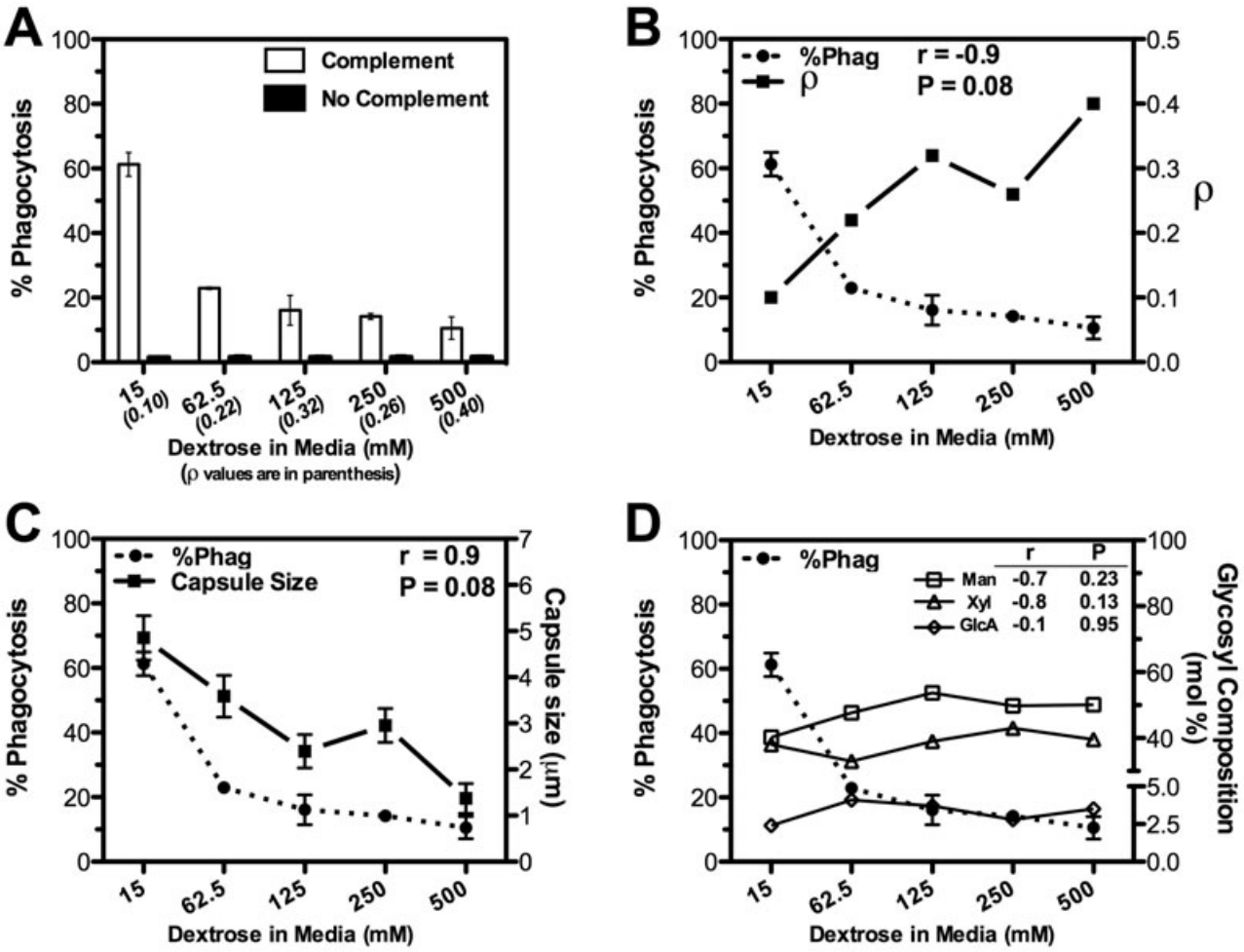

Fig. 5. Complement-mediated phagocytosis of cells grown in different dextrose concentrations.
A. Percentage of complement-mediated phagocytosis using H99 *C. neoformans* cells (as target cells) that were grown at different dextrose concentrations and exhibiting capsules with different degrees of PS branching.
B–D. These panels show the phagocytosis data from A analysed versus ρ of capsular PS, capsule size and glycosyl composition, respectively.

Effect of capsular PS branching in nitric oxide production. We investigated the reactivity of these structurally different PSs in stimulating or preventing NO production by phagocytes (Naslund *et al*., 1995; Chiapello *et al*., 2008; Xiao *et al*., 2008; Fonseca *et al*., 2010). For all samples, addition of capsular PS to macrophages-like cells yielded NO levels lower than in the media alone control condition (Fig. 6C). However, analysis of the dose–response effect showed differences in the ability of these PSs to inhibit NO production. An inhibitory response in NO production with increasing PS concentration was observed for capsular PS obtained from the culture supplemented with 15 mM of dextrose. This effect tended to shift (variable slopes) from a negative (15 mM), to neutral (125 mM), to a positive (500 mM) NO production response with increasing PS concentration. The NO inhibitory capacity of these PS samples was proportional to the ρ ($r = 1.0$, $P = 0.018$) (Fig. 6D). These results show that the inhibitory capacity of capsular PS to the production of NO by macrophage-like cells was dictated by polymer structure, such that the more branched PSs inhibited this process more efficiently.

Effect of capsular PS branching in protection against oxidative stress. Previous studies have shown that capsular PS can act as a buffer and protect cells against oxygen-derived oxidants (Zaragoza *et al*., 2008). We hypothesized that this capacity could be influenced by the degree of structural complexity of the PS molecules. Thus, we studied PSs exhibiting distinct degrees of branching in the ability to protect *Saccharomyces cerevisiae* cells from killing by H_2O_2. In the presence of cryptococcal capsular PS, yeast cells resulted to be less susceptible to the toxic effects of H_2O_2, confirming previous studies (Zaragoza *et al*., 2008). Moreover, distinct survival levels were evident depending on the degree of

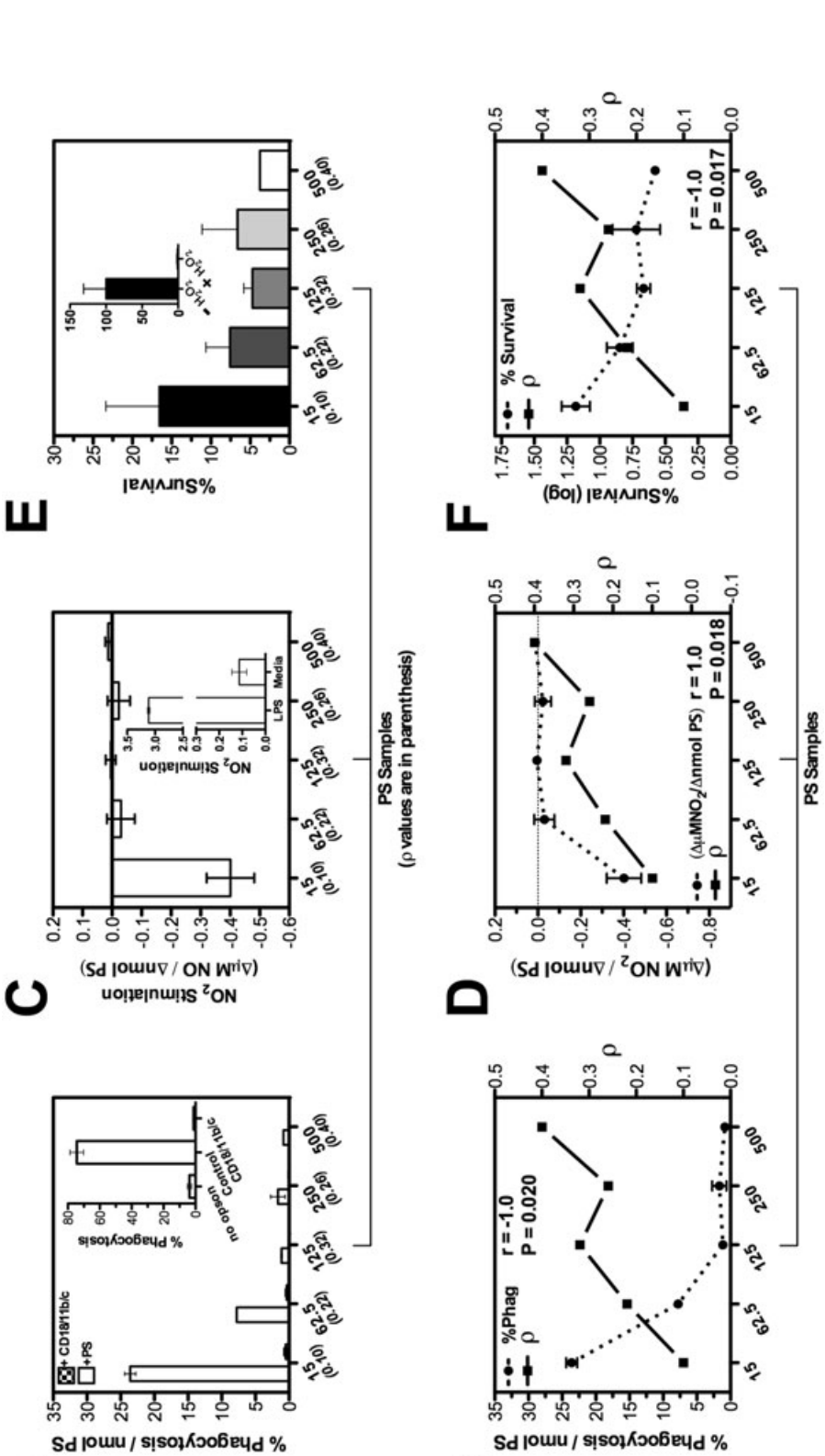

Fig. 6. Biological activity of capsular PS as a function of polymer structure. *C. neoformans* H99 capsular PS samples isolated (DMSO-extraction) from cells grown in cultures supplemented with different dextrose concentrations, which exhibited distinct degrees of polymer branching, were examined in their effect on (A) complement-mediated phagocytosis (C) NO production by macrophage-like cells, and (E) protection against hydrogen peroxide. The panels in the second row show the data from first row plotted for Spearman's analysis such panels (A, B) (C, D), and (E, F) are paired. (A) The efficiency of complement-mediated phagocytosis was inhibited in the presence of soluble PS and this effect correlated with PS branching. For each condition, antibodies against CD18, CD11b and CD11c, were added and their presence inhibited phagocytosis, establishing that ingestion proceeded by the complement receptor (filled bars). Inset shows percentage of phagocytosis for conditions where no PS was added and compares cells that were not opsonized, complement opsonized or complement opsonized plus CD18, CD11b and CD11c Abs) (B) Spearman correlation between percentage of phagocytosis and ρ of PS samples. (C) The inhibition capacity of NO production by soluble capsular PS samples tended to decrease as a function of PS branching. The *y*-axis in (C) and (D) is defined as the change in NO_2 concentration (μmolar) relative to the change in PS amount (nmoles). (D) Spearman correlation between NO production and ρ of PS samples. LPS and medium alone (no PS) were used as positive and negative controls (inset). (E) Protection to hydrogen peroxide by PS samples decreased as a function of PS branching. Data are presented as the percentage survival of *S. cerevisiae* cells relative to control (no H_2O_2). (F) Spearman correlation between percentage of survival and ρ of PS samples. For all panels, error bars represent standard deviations of mean values obtained from two experiments were each condition was tested in triplicates.

capsular PS structure complexity (Fig. 6E). The inverse correlation (Fig. 6F) (Spearman $r = -1.0$, $P = 0.017$) obtained between the percent survival and the ρ for each of the PS samples tested suggests that the ability of cryptococcal PS molecules to protect against oxidative stress was influenced by their structure, with less branched PSs being less efficient at protecting against oxidative fluxes.

Serum half-life depends on PS branching. We hypothesized that structural properties such as the degree of PS branching would influence the time required for its clearance in serum. To prove this, mice were injected intravenously with equivalent amounts of capsular PS samples differing in branching and serum levels were monitored over time by capture enzyme-linked immunoabsorbent assay (ELISA) (Fig. 7A). The half-life of capsular PS in serum strongly correlated with the degree of branching ($r = -1.0$, $P = 0.017$), such that the more branched (lowest ρ) PSs were cleared less rapidly (Fig. 7B).

Reactivity of anti-GXM monoclonal antibody. Because antibody epitope accessibility and/or distribution could also be greatly affected by structure, we sought to investigate the reactivity of two murine immunoglobulin M (IgM) mAbs (13F1 and 12A1) with PS that differed in branching. First, we performed direct immunofluorescence staining of H99 cells grown at different dextrose concentrations and producing capsular PS with distinct degrees of branching. In the case of mAb 13F1, qualitative differences in the binding pattern and intensity were difficult to analyse by microscopy because of mAb-mediated aggregations of yeasts cells. Interestingly, the frequency and size of these aggregates decrease as a function of PS branching (Fig. S3A). This correlation was confirmed by fluorescence-activated cell sorting (FACS) analysis (Fig. S3B and C). This effect was specific for 13F1 as no consistent differences were noticeable for mAb 12A1 (data not shown). In addition, the effect of PS branching on mAb 13F1 binding was investigated by ELISA using purified capsular PS (Fig. S3D). MAb 13F1 binding positively correlated with the branching degree of the PS; the highest binding signals were observed for the PS sample with the highest branching degree (lower ρ) and decreased with the less branched PS. No correlation was observed for mAb 12A1 (data not shown). Together, these results suggest that capsular PS branching and structure can influence antibody reactivity.

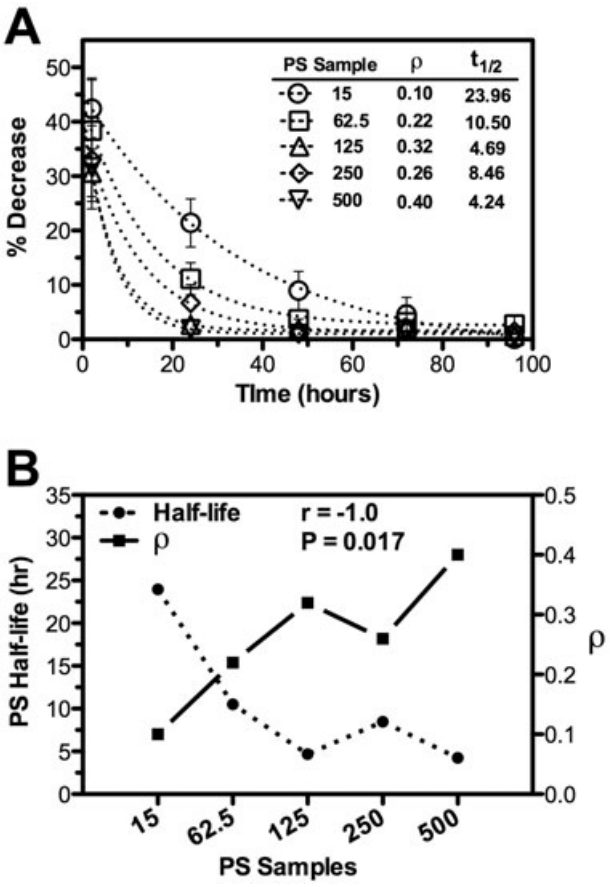

Fig. 7. PS clearance is influenced by PS structure. Mice ($n = 5$) were given 50 μg of soluble capsular PS samples isolated from *C. neoformans* H99 cells grown at different dextrose concentrations (15, 62.5, 125, 250, 500 mM) and exhibiting distinct branching degrees. Serum samples were collected at 2, 24, 48, 72 and 96 h post-I.V. administrations.
A. Percentage of GXM levels in serum was detected by capture ELISA. Each sample was analysed in duplicate.
B. The half-life (in hours) tended to increase as a function of PS branching. The error bars denote standard deviations.

Discussion

The *C. neoformans* capsular PS molecules have been presumed to be linear (Doering, 2009), but this inference made from absence of data to the contrary, as the question of PS branching for this fungal pathogen has never been explored experimentally. Although the xylose and glucuronic acid substitutions on the mannose backbone could technically be considered one-residue branches, to date there is no evidence for higher-order branched structures or information on the overall conformation of these polymers in solution. A challenge in studying cryptococcal PS is that most current biochemical, microscopic and conservation techniques have insufficient sensitivity to demonstrate complex branched polymers, largely because of the high degree of PS structure hydration, size and complexity of physical properties of the capsule (Cherniak *et al.*, 1998; McFadden *et al.*, 2007). Given that GXM polymers have masses in excess of 1 MDa, current methods of analytical chemistry cannot reliably detect rare sugar modifications indicative of branched structures

(Cherniak *et al.*, 1998). Nevertheless, it is possible to obtain evidence for or against polymer linearity from physical studies, such as LS (Burchard *et al.*, 1980).

The relationship between M_w and R_g parameters reported here was incompatible with a linear model. Cryptococcal PS exhibits very low size increments as a function of molecular mass, as reflected by the relative small scaling exponent (ν), similar to values observed for hyperbranched polymers (Millard *et al.*, 1999; Morris *et al.*, 2008). Importantly, we observed shared variances between M_w and R_g (good power fit R squared) values for samples before and after EDTA treatment. This suggests that although there is an associated overestimation of molecular parameters by aggregation, it is proportionate in such a way that it does not have a significant influence in our capacity to distinguish between linear or branched conformations. Another significant observation in our study was the striking differences between the R_h and R_g that were obtained among all the cryptococcal capsular PSs. These differences resulted in very low shape factors, regardless of EDTA treatment and the method of isolation, providing strong evidence for branching and a compacted conformation. Values such as these, which were lower than the one predicted for a compact monodisperse spheres (Burchard and Patterson, 1983), have also been observed for higher-order PS complexes such as microgels (Bello-Pérez *et al.*, 1998), where the polymer is formed by a compact highly cross-linked centre with numerous dangling chains at the surface. A more accurate description of PS conformation will require studies of cryptococcal PS by SLS and DLS, possibly after fractionation by a separation technique such as size exclusion chromatography. Although they appeared to be small, differences in ρ values between the different cryptococcal strains, divalent cation chelation and method of extraction were observed. As a result of the small scale, many of these differences can be considered significant and could reflect the expected structural variability of GXM polymers among strains, serotypes and method of analysis.

Our LS data for all capsular PSs demonstrated numerous characteristics resembling those observed for branched PSs. A curvature at high angles was observed for all cryptococcal capsular PSs, regardless of divalent cation chelation. This type of curvature reflects the structure-dependent angular behaviour of the scattering data approaching a spherical shape (Nordmeier, 1993). While random coils (having a Flory distribution of molar mass) gives straight lines (Nordmeier, 1993), branched polymers produce such curved patterns, as is the case for dextran (Nordmeier, 1993) and amylopectin (Millard *et al.*, 1999; Zhong *et al.*, 2006), the latter being a high M_w and hyperbranched PS (Burchard and Patterson, 1983). In general, chelation of divalent cations reduced cryptococcal PS M_w, R_g and R_h values. This observation is consistent with the known ability of GXM molecules to self-aggregate (Nimrichter *et al.*, 2007), thus resulting in some overestimation of size and mass.

The idea of a high-order branched conformation was supported by rheological analysis of capsular PS solutions. While amylopectin and pullulan exhibited simple Newtonian flow, H99 capsular PS showed shear-thinning behaviour at the same PS concentration, consistent with the presence of highly entangled polymers. This result showed that cryptococcal capsular PS molecules, even at very low concentrations and in the presence of salt, exhibit significant inter-molecular interactions, a finding that is consistent with a complex structure and strong capacity of GXM molecules to self-associate (McFadden *et al.*, 2006a,b).

Visual evidence of capsular PS branching and compact structure was obtained using high-resolution microscopy. The negatively stained TEM images of capsular PS isolated from *C. neoformans* H99 cells revealed spherical rosette-like particles reminiscent of structures described for liver glycogen (Childress *et al.*, 1970; Cruz, 2004) and TM3a, a branched PS from *Pleurotus tuber-regium* (Tao *et al.*, 2007). This result strongly supports the notion that the structure of cryptococcal capsular PS is branched, a finding that is consistent with our LS data.

A number of studies have suggested that PS fractions obtained from species belonging to the *Cryptococcus* complex show enormous structural variability, which is apparently linked to the biological activities of cryptococcal capsular components (Cherniak *et al.*, 1998; Charlier *et al.*, 2005; McFadden *et al.*, 2006b; Nimrichter *et al.*, 2007; Frases *et al.*, 2008; De Jesus *et al.*, 2010; Fonseca *et al.*, 2010). More specifically, exo-PS samples from similar cryptococcal species are diverse in their ability to stimulate cellular responses, which is apparently related to the hydrodynamic effective diameter of GXM molecules (Fonseca *et al.*, 2010). In addition, the hydrodynamic size is also a determinant for serological recognition of PS by monoclonal antibodies (Nimrichter *et al.*, 2007; Frases *et al.*, 2008). As this measurement of apparent size is dependent on the M_w and shape of the particle in solution, it is difficult to discriminate magnitude versus conformation as the predictor for such biological effects. Yet, these results established the potential of physical chemical properties of PS fractions to modulate the host response (Fonseca *et al.*, 2010). Hence, we hypothesized that the extent of PS branching would influence the biological properties of *C. neoformans* PS. To test this hypothesis, we needed conditions where we could vary the PS branching while retaining comparable monosaccharide compositions. Recently, we observed that the structure of the PS capsule was modulated by carbon sources in a concentration-dependent manner, as suggested by differences in their hydrodynamic sizes (Guimaraes *et al.*,

2010), and used this approach to generate PS with variable structural properties. To test whether these effects altered capsule complexity or branching, we examined the shape of polymer molecules derived from capsules of cells grown in different dextrose concentrations to infer the state of polymer branching.

The sugar composition of the different capsular PS samples was each very similar, a finding that would have implied similar chemical–physical properties assuming linear/simple structures. However, all five samples had ρ values less than one, suggestive of, and consistent with, the existence of highly branched structures and compacted polymer conformations. A significant correlation of ρ and intrinsic viscosity with the dextrose concentration used in the media was observed, consistent with different degrees of branching. Analysis of these samples demonstrated that PS conformation is an important phenotypic characteristic in *C. neoformans* biology. The ability of capsular PSs to inhibit phagocytosis and NO production by macrophage-like cells, protect against reactive oxygen species, react with mAb 13F1 and modify their half-life in serum depended on the degree of branching, highlighting the important relation between structure and functionality. With regards to phagocytosis, the results obtained with isolated polysaccharide preparations correlated closely with the observations on whole cells. This observation is consistent with and supports the view that the effects in complement-mediated phagocytosis obtained with cryptococcal cells grown in different amounts of dextrose were a result of expressing capsules with differences in polysaccharide branching.

The structure and chain conformations of PS molecules and the importance of these characteristics on their biological activities are not unique for cryptococcal PSs (Riccio *et al*., 1996; Tao *et al*., 2007; Yang and Zhang, 2009). For example, the hyperbranched fungal PSs TM3a is produced by *Pleurotus tuber-regium* (Tao and Zhang, 2006; Tao *et al*., 2007) and *Coriolus versicolor* synthesizes coriolan (Miyazaki *et al*., 1974), both of which produce immunomodulatory activities (Ng, 1998; Tao *et al*., 2006). Moreover, lentinan, a branched PS produced by *Lentinus edodes* (Chihara *et al*., 1969; Sasaki and Takasuka, 1976), is a good example of the structure–activity relationship in PSs. With two β-(1→6)-glucopyranoside branches for every five β-(1→3)-glucopyranoside backbone (Sasaki and Takasuka, 1976), this PS can exist as a linear, circular, branched triple-helical or random-coil chains depending on solvent and temperature (Zhang *et al*., 2004). Lentinan also has immunomodulatory activity, and its antitumor effects depend on the PS chain conformation (Ohno *et al*., 1995; Zhang *et al*., 2005).

Our results provide strong evidence that *C. neoformans* capsular PSs are branched, with molecules forming compacted structures that could arise by biochemical synthesis of a modified branched sugar or, more likely, cross-linking of PS molecules. This characteristic seems to play an important regulator of complement-mediated phagocytosis, nitric oxide production by phagocytes, protection against reactive oxygen species, antibody reactivity and the half-life of PS in the serum. A PS capsule composed of branched PS structures has no precedent in the literature of the medical microbiology field as the capsular PS of well-characterized encapsulated microbes such as *Streptococcus pneumoniae*, *Haemophilus influenzae* and *Neisseria meningitidis* are unbranched homopolymers. Such complexity in cryptococcal PS structure relative to bacteria is perhaps not unexpected, because the pathways involved in synthesis and cellular traffic of PSs of eukaryotic microbes differ from those of prokaryotes. For example, GXM is synthesized in the Golgi (Yoneda and Doering, 2006) and shed by a vesicular transport system (Rodrigues *et al*., 2007). According to our data, branching of PS would be also expected to have major consequences for the interaction of *C. neoformans* with the immune system as well as immunogenicity. The evidence for branching suggests the need for future biochemical studies to identify modified sugars that can serve as synthetic branch points or the mechanisms by which distinct PS molecules may be linked to produce such complex structures. Hence, our observations provide new research directions for the cryptococcal field and capsule studies that can be correlated with different modifications of the *C. neoformans* capsule.

Experimental procedures

Yeast strains and growth conditions

Cryptococcus neoformans Serotype A strain H99 (American Type Culture Collection (ATCC) 208821), Serotype B strains NIH 191 and NIH 444 (ATCC 32609), Serotype C strain 106.93, Serotype strains D ATCC 24067 and B-3501 (ATCC 34873) and Serotype AD strain MAS92-203 were grown for 48 h at 30°C in capsule inducing media composed of: 10 mM $MgSO_4$, 29.3 mM KH_2PO_4, 13 mM glycine, 3 μM thiamine-HCl; adjusted to pH 5.5 and supplemented with 15 mM (regular minimal media) dextrose as the solely carbon source. For some experiments, minimal media was supplemented with 62.5, 125, 250 or 500 mM of dextrose as the carbon source.

Polysaccharide samples

Capsular PS was isolated as described previously (Bryan *et al*., 2005). Briefly, yeast cells were washed three times with distilled water and collected by centrifugation. Wet cell pellets were suspended in 15 ml of dimethyl sulfoxide (DMSO) and incubated for 30 min. The cells were spun down by centrifugation and the DMSO supernatant was then dialysed against

distilled water for 12 h, with water replacement every 2 h. Samples were then extensively dialysed against distilled water or against 1 mM EDTA for 3 days. After this time, PS solutions were lyophilized (DMSO-PS). For some experiments, cryptococcal PS were isolated from 24067 strain using different methods such as cetyltrimethylammonium bromide precipitation (CTAB-PS), ultrafiltration (F-PS) and gamma radiation (GR-PS) as described (Frases *et al.*, 2008). Amylopectin (from maize), glycogen (from slipper limpet-Type VIII), amylose (from potato) and pullulan (1600 kDa) were purchased from Sigma-Aldrich and used as standards for structural studies.

Measurement of molecular weight (M_w) and Radius of gyration (R_g) by Static LS

The M_w and R_g were measured by SLS using a differential refractometer and molecular weight analyser (BI-DNDC, BI-MwA, respectively; Brookhaven Instruments, Hotsville, NY, USA). Lyophilized PSs samples were suspended in sterile-filtered, degassed ultra-pure water with 10 mM NaCl at 1 mg ml^{-1}, followed by extensive agitation and overnight incubations at 60°C for three consecutive days. All PS solutions were filtered through a 0.8 μm syringe filter and equilibrated to 25°C before testing. Capsular PS solutions were prepared at different concentrations (1–7 μg ml^{-1}) and confirmed by the phenol sulfuric acid colorimetric method (DuBois *et al.*, 1956). Differential refractometry was done using a 620 nm laser source to measure the change in refractive index as a function of concentration (*dn/dc*) of the PS samples. Average M_w and R_g were determined at 25°C by multi-angle laser (static) LS using a 675 nm laser source. Rayleigh scattering intensities collected at 35, 50, 75, 90, 105, 130, 145° angles were analysed using Berry plots, which is given by the equation: $Kc/R_q = (1 + A_2M_wc)^2/\{M_wP(q)\}$. The Berry extrapolation procedure was used rather than classic Zimm extrapolation because it enables a more accurate mathematical transformation of the LS function for polymers of large molecular mass (Aberle *et al.*, 1994; Andersson *et al.*, 2003; Rolland-Sabate *et al.*, 2007). Because of the curvature of the obtained plots, a 2nd order polynomial was used to fit the data. Good reproducibility was obtained for all PS samples based on duplicate measurements.

Hydrodynamic radius (R_h) and polydispersity of PS samples by dynamic LS

The R_h and polydispersity of PS preparations were measured by DLS in a 90Plus/BI-MAS Multi Angle Particle Sizing analyser (Brookhaven Instruments) as described (Frases *et al.*, 2009). PS sample solutions were prepared as described above. The fluctuating signals, originating from the random motion of particles in solution and the associated alterations in the intensity of the scattered light over time, were processed by the autocorrelation function, $C(t)$, $C(t) = Ae^{2\Gamma t} + B$; where t is the time delay, A is an optical constant, and Γ equals $D^{1/2}q$. The value of q is calculated from the scattering angle θ, the wavelength of the laser light λ_0, and the index of refraction n of the suspended liquid, according to the equation $q = \left(\frac{2\pi n}{\lambda_0}\right)2\sin\left(\frac{\theta}{2}\right)$. Particle size is related to the translational diffusion coefficient (D) as a function of molecular shape, defined by $D = \frac{K_BT}{3\pi\eta(t)d}$; where K_B is Boltzmann's constant (1. 38054×10^{-16} erg/K), T is the temperature (303 K), $\eta(t)$ is the viscosity of the suspension liquid and d is the particle diameter. Polydispersity or the relative standard deviation of the sample, is defined as $\frac{\mu_2}{\Gamma^2}$, where μ_2 is proportional to the variance of the intensity-weighted distribution. Average R_h was calculated from duplicates of 10 individual measurements. The multimodal size distributions of particles diameter were obtained by a Non-Negatively constrained Least Squares algorithm (NNLS) based on the intensity of light scattered by each particle. All PS samples were analysed under the same conditions.

Microscopy

Negative stain electron microscopy of isolated PS. Purified PS were transferred to formvar-carbon coated grids and negatively stained with 1% phosphotungstic acid. The grids were then blotted dry immediately before observing in a JEOL 100CX II transmission electron microscope (JEOL USA) at 80 kV. Diameter of 100 structures from 10 different fields was measured in ImageJ 1.39u software (National Institutes of Health).

Scanning Electron Microscopy (SEM) of C. neoformans *cells.* Yeast cells were fixed in 2.5% glutaraldehyde, 0.1 M sodium Cacodylate, 0.2 M sucrose and 5 mM $MgCl_2$ at pH 7.4. Sample was then dehydrated through a graded series of ethanol. Critical point dry was done using liquid carbon dioxide in a Tousimis Samdri 795 Critical Point drier (Rockville, MD, USA). Sputter was coated with gold-palladium in a Denton Vacuum Desk-2 Sputter Coater (Cherry Hill, NJ, USA). Samples were visualized in a JEOL JSM6400 Scanning Electron Microscope (Peabody, MA, USA) using an accelerating voltage of 10 KV.

Capsule size measurements. H99 *C. neoformans* cells were mixed with a drop of India-ink (BD Biosciences, Franklin Lakes, NJ, USA) and visualized using an Olympus AX 70 microscope (Melville, NY, USA). Capsule size was measured in ImageJ 1.40 g software (National Institutes of Health NIH, Bethesda, MD, USA) considering the distance from the cell wall and the India-ink exclusion zone. Average and standard deviation from at least 100 measurements were calculated.

Glycosyl composition of PS. PS samples were processed as previously described (York *et al.*, 1985; Merkle and Poppe, 1994). Briefly, PS fractions were dissolved in methanol with 1 M HCl and incubated at 80°C for 18 h. Inositol was used as the internal standard. Methanolyzed samples were then per-*O*-trimethylsilylated by treatment with Tri-Sil (Pierce) for 30 min at 80°C. The per-*O*-trimethylsilylated methyl glycosides derivatives were analysed by gas chromatography coupled to mass spectrometry (GC/MS) on an HP 5890 gas

chromatograph interfaced to a 5975B MSD mass spectrometer, using a Supelco DC-1 fused silica capillary column (30 m × 0.25 mm ID). Both derivatization and GC/MS of standard sugar mixtures were done in parallel with the experimental samples. Carbohydrate standards included arabinose, rhamnose, fucose, xylose, glucuronic acid, galacturonic acid, mannose, galactose, dextrose, mannitol, dulcitol and sorbitol. Analysis of the differences in sugar composition between capsular PS samples was performed by comparing the mole percentages of Xyl, Man and GlcA between the five samples using a repeated measure test one-way ANOVA.

Viscosity. The viscosity profiles of capsular PS samples isolated (by DMSO extraction) from an H99 culture grown in minimal media were investigated by a stress-controlled steady shear experiment. PS solutions were prepared at different concentrations (1, 0.1, 0.075, 0.05, 0.025 mg ml^{-1}) as described for the static LS studies. Rotational rheological measurements were conducted at 25°C using a NOVA Rheometer with ETC-2 Joule-Thomson Effect Temperature Cell in a 40 mm diameter parallel plate fixture with a fixed 0.3 mm gap. A constant 10.0 N normal loading force was used to ensure exact sample loading history. Intrinsic viscosity of the capsular PS samples isolated from H99 *C. neoformans* cultures grown at increasing dextrose concentrations were measured using a modified Ostwald-type capillary glass viscometer (Cannon-Manning Semi-Micro, Technical Glass, Dover, NJ) in a temperature-controlled water bath at 25°C. Different concentrations of PS solutions were prepared as described. Flow times were measured in triplicate. Relative viscosity was calculated as the change in the ratio of the flow time of the sample to the solvent, $\left(\eta = \frac{\eta}{\eta_0}\right)$. The intrinsic viscosity, ($\eta_{sp} = \eta - \eta_0 = \eta_{sp} - 1$), was calculated by normalizing η_{sp} to concentration and extrapolating this value to zero concentration $\left(|\eta| = \lim_{C \to 0} \frac{\eta_{sp}}{C}\right)$.

Nitric oxide production. Murine macrophage-like cell line J774.16 was cultivated in complete Dulbecco's Modified Eagle Medium (DMEM) composed of 10% heat-inactivated (56°C for 30 min) fetal calf serum (Gemini Bio-products, Woodland, CA, USA), 10% NCTC-109 medium (Gibco) and 1% MEM non-essential amino acids (Gibco-Invitrogen 11360), at 37°C in a 10% CO_2 atmosphere. Capsular PSs isolated from *C. neoformans* H99 cells grown in different concentrations of dextrose were suspended in DMEM. Decreasing concentration of capsular PSs (0.500, 0.250, 0.125, 0.062.5, 0.031.25 nM in DMEM) were added to wells in 1 ml total volumes (24-well tissue culture plates) containing 1×10^6 macrophages and incubated for 16 h at 37°C in a 10% CO_2 atmosphere. After incubation, supernatants were collected followed by quick centrifugation step to ensure clearance of any type of cell debris. NO production was analysed as depicted by Griess Reagent System (Promega, Madison, WI, USA). Macrophages-like cells stimulated with 0.5 μg ml^{-1} lipopolysaccharide (LPS) or in the absence of PS were used as controls. NO production was calculated as the change in NO_2 concentration relative to the change in PS amount (in nmoles). Experiments were performed in triplicate sets.

Phagocytosis assay. Approximately 5×10^4 J774.16 macrophage-like cells/well were plated in complete DMEM, and incubated overnight at 37°C in a 10% CO_2 atmosphere. Cells were continuously kept under the stimulation of recombinant murine γ-interferon (IFN-γ) and LPS; 100 U ml^{-1} and 0.5 ug ml^{-1} respectively. *C. neoformans* H99 cells grown for 48 h under different dextrose concentrations were washed with PBS (3×), and resuspended in DMEM supplemented with 20% mouse sera (Pel-Freez Biologicals, Rogers, AR, USA), incubated for 20 min and subsequently added to macrophage monolayer in 1:5 (macrophage : yeast) ratio. Unopsonized yeast cells resuspended in DMEM (lacking mouse sera) were used as control. After 1.5 h incubation at 37°C the macrophage monolayer was washed three times with PBS, fixed with cold methanol, and stained with 1:5 solution of Giemsa in distilled water. The percentage of phagocytosis was determined by microscopic examination of the number of macrophages with internalized and attached yeast cells divided by total macrophages. For each condition, at least 300 macrophage cells were analysed. Experiments were done in triplicate sets. To measure the ability of isolated capsular PS to inhibit phagocytosis of complement-opsonized yeast cells, capsular PS samples isolated from *C. neoformans* H99 cells grown in different concentrations of dextrose and expressing distinct branching degrees were suspended in DMEM and used to a final concentration of 2.5 nM. PS solutions (100 μl) were added to macrophages and incubated for 30 min at 37°C in 10% CO_2. As a control, complement-mediated phagocytosis was blocked with antibodies against CD18, CD11b and CD11c (each at 10 μg ml^{-1}) (BD Pharmingen, San Diego, CA, USA). *C. neoformans* H99 cells grown in Sabouraud's media for 48 h (target cells), washed 3× with PBS and resuspended in DMEM supplemented with 20% mouse sera, incubated for 20 min and subsequently added to macrophages resulting in a final 1:5 (macrophage : yeast) ratio. Determination of percentage of phagocytosis was performed as described above.

Reactive-oxygen species protection assay. The ability of capsular PS expressing distinct degrees of structure complexity to protect *S. cerevisiae* yeast cells from oxidative stress was determined (Zaragoza *et al.*, 2008). Briefly, a suspension of 2×10^3 cells ml^{-1} cells (BY strain) in water was treated with 0.5 mM hydrogen peroxide with or without the presence (DMSO-extracted) capsular PS (5 nM final concentration). Capsular PS samples isolated from H99 *C. neoformans* cells grown at different dextrose concentrations were used for this experiment. Each sample was done in quadruplicates. After 2 h incubation at 30°C, 50 or 100 μL of the cell suspensions was spread-inoculated in Sabouraud agar plates and incubated at 30°C for 48 h. Percent of survival was determined by counting the number of colony forming units relative to the control condition (no H_2O_2 added).

Capsular PS clearance. Intravascular clearance of capsular PS samples isolated from H99 cells grown at different dextrose concentrations and exhibiting distinct degrees of PS branching were determined by capture ELISA after tail-vein injection (50 μg in 100 μl) to BALB/c mice (National Cancer

Institute) ($n = 5$). Blood samples were collected by retro-orbital bleeding of mice at different times post-injection (2, 24, 48, 72 and 96 h). Serum was collected by centrifugation of blood samples at 2000 r.p.m. for 10 min. Capsular PS levels in the serum were determined by capture ELISA as previously described (Casadevall *et al.*, 1992) using mAb 2D10 (IgM) for capture and mAb 18B7 for detection. In order to minimize non-specific activity, serum samples were incubated with proteinase K at 37°C overnight and heat inactivated in boiling water for 10 min. Each sample was measured in duplicate. Data are represented as the percentage decrease of PS concentration relative to initial dose. PS half-life was calculated by: ln(2)/*K*, were *K* is the rate constant obtained by fitting the data to a one phase decay equation.

Reactivity with GXM-monoclonal antibodies. H99 cells (1×10^6) grown in different dextrose concentrations were washed three times with PBS and suspended in blocking solution (2% (w/v) bovine serum albumin in TBS-T; 10 mM Tris-HCl, 150 mM NaCl, 1 mM NaN_3, 0.1% Tween 20, pH 7.4) containing 10 μg ml^{-1} of mAb 13F1 or 12A1. Cell wall was detected with Uvitex 2B (Polysciences, Warrington, PA, USA). All incubations were done for 1 h at 37°C. Cell suspensions were washed (PBS 3×) and examined under fluorescent filters with the Olympus AX70 microscope, using QCapture Suite V2.46 software. Size and frequency of aggregates was confirmed by monitoring the forward side scatter (FSC) in a FACScan Flow Cytometer (BD Biosciences). For ELISA experiments, a 96-well polystyrene plate was coated with isolated (by DMSO) capsular PS (15–500 mM) samples diluted in PBS with concentrations ranging from 1 mg ml^{-1} to 5.64 ng ml^{-1} (obtained by 1:3 serial dilutions). After washed with TBS-T (3×), wells were incubated with 50 ul of 10 μg ml^{-1} mAb 13F1 or 12A1, followed by detection with 1:1000 dilution of anti-IgM-AP antibody. All samples were done in replicates of four and all incubations were done for 1 h at 37°C.

Statistical analysis. Statistical analyses were carried in Bi-ZPMwA Zimm Plot Software (Brookhaven Instruments). 90Plus/BI-MAS Software was used for effective diameter and polydispersity parameters (Brookhaven Instruments). Plots, curve fits, Pearson or Spearman correlations (r), and statistical analysis were performed using GraphPad Prism version 5.0a, GraphPad Software, San Diego, California, USA.

Acknowledgements

Funding for this project was supported by NIH awards AI033774, HL059842 and AI033142. RJBC was supported by the Training Program in Cellular and Molecular Biology and Genetics, T32 GM007491. Carbohydrate and NMR analyses were performed at the Complex Carbohydrate Research Center, University of Georgia, Atlanta, which is supported in part by the Department of Energy-funded (DE-FG-9-93ER-20097) Center for Plant and Microbial Complex Carbohydrates. We thank Marcio L. Rodrigues, Joshua D. Nosanchuk, Antonio Nakouzi and Luis R. Martinez for critical reading of the manuscript and giving us helpful suggestions and comments. We thank Ignacio Guerrero Ros for his assistance in the capsular PS clearance experiments.

References

Aberle, T., Burchard, W., Vorwerg, W., and Radosta, S. (1994) Conformational contributions of amylose and amylopectin to the structural properties of starches from various sources. *Starch/Stärke* **46:** 329–335.

Andersson, M., Wittgren, B., and Wahlund, K.G. (2003) Accuracy in multiangle light scattering measurements for molar mass and radius estimations. Model calculations and experiments. *Anal Chem* **75:** 4279–4291.

Bacon, B.E., Cherniak, R., Kwon-Chung, K.J., and Jacobson, E.S. (1996) Structure of the O-deacetylated glucuronoxylomannan from *Cryptococcus neoformans* Cap70 as determined by 2D NMR spectroscopy. *Carbohydr Res* **283:** 95–110.

Bello-Pérez, L.A., Colonna, P., Roger, P., and Octavio, P.-L. (1998) Laser light scattering of high amylose and high amylopectin materials in aqueous solution, effect of storage time. *Carbohyd Polym* **37:** 383–394.

Bryan, R.A., Zaragoza, O., Zhang, T., Ortiz, G., Casadevall, A., and Dadachova, E. (2005) Radiological studies reveal radial differences in the architecture of the polysaccharide capsule of *Cryptococcus neoformans*. *Eukaryot Cell* **4:** 465–475.

Burchard, W., and Patterson, G.D. (1983) *Light Scattering from Polymers*. Berlin; NY: Springer-Verlag, p. 167.

Burchard, W., Schmidt, M., and Stockmayer, W.H. (1980) Information on polydispersity and branching from combined quasi-elastic and intergrated scattering. *Macromolecules* **13:** 1265–1272.

Casadevall, A., Mukherjee, J., and Scharff, M.D. (1992) Monoclonal antibody based ELISAs for cryptococcal polysaccharide. *J Immunol Methods* **154:** 27–35.

Chang, Y.C., and Kwon-Chung, K.J. (1994) Complementation of a capsule-deficient mutation of *Cryptococcus neoformans* restores its virulence. *Mol Cell Biol* **14:** 4912–4919.

Charlier, C., Chretien, F., Baudrimont, M., Mordelet, E., Lortholary, O., and Dromer, F. (2005) Capsule structure changes associated with *Cryptococcus neoformans* crossing of the blood-brain barrier. *Am J Pathol* **166:** 421–432.

Cherniak, R., and Sundstrom, J.B. (1994) Polysaccharide antigens of the capsule of *Cryptococcus neoformans*. *Infect Immun* **62:** 1507–1512.

Cherniak, R., Valafar, H., Morris, L.C., and Valafar, F. (1998) *Cryptococcus neoformans* chemotyping by quantitative analysis of 1H nuclear magnetic resonance spectra of glucuronoxylomannans with a computer-simulated artificial neural network. *Clin Diagn Lab Immunol* **5:** 146–159.

Chiapello, L.S., Baronetti, J.L., Garro, A.P., Spesso, M.F., and Masih, D.T. (2008) *Cryptococcus neoformans* glucuronoxylomannan induces macrophage apoptosis mediated by nitric oxide in a caspase-independent pathway. *Int Immunol* **20:** 1527–1541.

Chihara, G., Maeda, Y., Hamuro, J., Sasaki, T., and Fukuoka, F. (1969) Inhibition of mouse sarcoma 180 by polysaccharides from *Lentinus edodes* (Berk.) sing. *Nature* **222:** 687–688.

Childress, C.C., Sacktor, B., Grossman, I.W., and Bueding, E. (1970) Isolation, ultrastructure, and biochemical characterization of glycogen in insect flight muscle. *J Cell Biol* **45:** 83–90.

Cleare, W., and Casadevall, A. (1999) Scanning electron

microscopy of encapsulated and non-encapsulated *Cryptococcus neoformans* and the effect of glucose on capsular polysaccharide release. *Med Mycol* **37:** 235–243.
Cruz, A.F. (2004) Element storage in spores of Gigaspora margarita Becker & Hall measured by electron energy loss spectroscopy (EELS). *Acta Botanica Brasilica* **18:** 473–480.
Davis, K.A., Ackerson, B.J., Yu, H., Ford, W.T., Xia, J., and Dubin, P.L. (1994) Structure and transport of Latex microgels in aqueous suspension. *Langmuir* **10:** 2145–2150.
De Jesus, M., Chow, S.K., Cordero, R.J., Frases, S., and Casadevall, A. (2010) Galactoxylomannans from *Cryptococcus neoformans* varieties neoformans and grubii are structurally and antigenically variable. *Eukaryot Cell* **9:** 1018–1028.
Doering, T.L. (2000) How does *Cryptococcus* get its coat? *Trends Microbiol* **8:** 547–553.
Doering, T.L. (2009) How sweet it is! Cell wall biogenesis and polysaccharide capsule formation in *Cryptococcus neoformans*. *Annu Rev Microbiol* **63:** 223–247.
Dong, Z.M., and Murphy, J.W. (1995) Effects of the two varieties of *Cryptococcus neoformans* cells and culture filtrate antigens on neutrophil locomotion. *Infect Immun* **63:** 2632–2644.
DuBois, M., Gilles, K.A., Hamilton, J.K., Rebers, P.A., and Smith, F. (1956) Colorimetric Method for Determination of Sugars and Related Substances. *Anal Chem* **28:** 350–356.
Dykstra, M.A., Friedman, L., and Murphy, J.W. (1977) Capsule size of *Cryptococcus neoformans*: control and relationship to virulence. *Infect Immun* **16:** 129–135.
Eisenman, H.C., Frases, S., Nicola, A.M., Rodrigues, M.L., and Casadevall, A. (2009) Vesicle-associated melanization in *Cryptococcus neoformans*. *Microbiology* **155:** 3860–3867.
Ferry, J. (1980) *Viscoelastic Properties of Polymers*. New York: John Wiley & Sons.
Fonseca, F.L., Nohara, L.L., Cordero, R.J., Frases, S., Casadevall, A., Almeida, I.C., *et al*. (2010) Immunomodulatory effects of serotype B glucuronoxylomannan from *Cryptococcus* gattii correlate with polysaccharide diameter. *Infect Immun* **78:** 3861–3870.
Frases, S., Nimrichter, L., Viana, N.B., Nakouzi, A., and Casadevall, A. (2008) *Cryptococcus neoformans* capsular polysaccharide and exopolysaccharide fractions manifest physical, chemical, and antigenic differences. *Eukaryot Cell* **7:** 319–327.
Frases, S., Pontes, B., Nimrichter, L., Viana, N.B., Rodrigues, M.L., and Casadevall, A. (2009) Capsule of *Cryptococcus neoformans* grows by enlargement of polysaccharide molecules. *Proc Natl Acad Sci USA* **106:** 1228–1233.
Grijpstra, J., Gerwig, G.J., Wosten, H., Kamerling, J.P., and de Cock, H. (2009) Production of extracellular polysaccharides by CAP mutants of *Cryptococcus neoformans*. *Eukaryot Cell* **8:** 1165–1173.
Guimaraes, A.J., Frases, S., Cordero, R.J., Nimrichter, L., Casadevall, A., and Nosanchuk, J.D. (2010) *Cryptococcus neoformans* responds to mannitol by increasing capsule size in vitro and in vivo. *Cell Microbiol* **12:** 740–753.
Hanselmann, R., Burchard, W., Ehrat, M., and Widmer, H.M. (1996) Structural properties of fractionated starch polymers and their dependence on the dissolution process. *Macromolecules* **29:** 3277–3282.
Heiss, C., Klutts, J.S., Wang, Z., Doering, T.L., and Azadi, P. (2009) The structure of *Cryptococcus neoformans* galactoxylomannan contains beta-D-glucuronic acid. *Carbohydr Res* **344:** 915–920.
Kozel, T.R., and Gotschlich, E.C. (1982) The capsule of *cryptococcus neoformans* passively inhibits phagocytosis of the yeast by macrophages. *J Immunol* **129:** 1675–1680.
Kozel, T.R., and Mastroianni, R.P. (1976) Inhibition of phagocytosis by cryptococcal polysaccharide: dissociation of the attachment and ingestion phases of phagocytosis. *Infect Immun* **14:** 62–67.
Kozel, T.R., Gulley, W.F., and Cazin, J., Jr (1977) Immune response to *Cryptococcus neoformans* soluble polysaccharide: immunological unresponsiveness. *Infect Immun* **18:** 701–707.
Larsen, R.A., Pappas, P.G., Perfect, J., Aberg, J.A., Casadevall, A., Cloud, G.A., *et al*. (2005) Phase I evaluation of the safety and pharmacokinetics of murine-derived anticryptococcal antibody 18B7 in subjects with treated cryptococcal meningitis. *Antimicrob Agents Chemother* **49:** 952–958.
McClelland, E.E., Bernhardt, P., and Casadevall, A. (2005) Coping with multiple virulence factors: which is most important? *PLoS Pathog* **1:** e40.
McFadden, D., Zaragoza, O., and Casadevall, A. (2006a) The capsular dynamics of *Cryptococcus neoformans*. *Trends Microbiol* **14:** 497–505.
McFadden, D.C., De, M., and Casadevall, A. (2006b) The physical properties of the capsular polysaccharides from *Cryptococcus neoformans* suggest features for capsule construction. *J Biol Chem* **281:** 1868–1875.
McFadden, D.C., Fries, B.C., Wang, F., and Casadevall, A. (2007) Capsule structural heterogeneity and antigenic variation in *Cryptococcus neoformans*. *Eukaryot Cell* **6:** 1464–1473.
Macher, A.M., Bennett, J.E., Gadek, J.E., and Frank, M.M. (1978) Complement depletion in cryptococcal sepsis. *J Immunol* **120:** 1686–1690.
Merkle, R.K., and Poppe, I. (1994) Carbohydrate composition analysis of glycoconjugates by gas-liquid chromatography/mass spectrometry. *Methods Enzymol* **230:** 1–15.
Millard, M.M., Wolf, W.J., Dintzis, F.R., and Willett, J.L. (1999) The hydrodynamic characterization of waxy maize amylopectin in 90% dimethyl sulfoxide-water by analytical ultracentrifugation, dynamic, and static light scattering. *Carbohyd Polym* **39:** 315–320.
Miyazaki, T., Yadomae, T., Sugiura, M., Ito, H., and Fujii, K. (1974) Chemical structure of antitumor polysaccharide, coriolan, produced by *Coriolus versicolor*. *Chem Pharm Bull* **22:** 1739–1742.
Morris, G.A., Ang, S., Hill, S.E., Lewis, S., Sch‰fer, B., Nobbmann, U., and Harding, S.E. (2008) Molar mass and solution conformation of branched [alpha](1†–>†4), [alpha](1†–>†6) Glucans. Part I: glycogens in water. *Carbohyd Polym* **71:** 101–108.
Murakami, T., Uchida, S., and Ishizu, K. (2008) Architecture of hyperbranched polymers consisting of a stearyl methacrylate sequence via a living radical copolymerization. *J Colloid Interface Sci* **323:** 242–246.

Murphy, J.W., and Cozad, G.C. (1972) Immunological unresponsiveness induced by cryptococcal capsular polysaccharide assayed by the hemolytic plaque technique. *Infect Immun* **5:** 896–901.

Naslund, P.K., Miller, W.C., and Granger, D.L. (1995) *Cryptococcus neoformans* fails to induce nitric oxide synthase in primed murine macrophage-like cells. *Infect Immun* **63:** 1298–1304.

Ng, T.B. (1998) A review of research on the protein-bound polysaccharide (polysaccharopeptide, PSP) from the mushroom *Coriolus versicolor* (Basidiomycetes: Polyporaceae). *Gen Pharmacol* **30:** 1–4.

Nilsson, L., Leeman, M., Wahlund, K.G., and Bergenstahl, B. (2006) Mechanical degradation and changes in conformation of hydrophobically modified starch. *Biomacromolecules* **7:** 2671–2679.

Nimrichter, L., Frases, S., Cinelli, L.P., Viana, N.B., Nakouzi, A., Travassos, L.R., *et al*. (2007) Self-aggregation of *cryptococcus neoformans* capsular glucuronoxylomannan is dependent on divalent cations. *Eukaryot Cell* **6:** 1400–1410.

Nordmeier, E. (1993) Static and dynamic light-scattering solution behavior of pullulan and dextran in comparison. *J Phys Chem* **97:** 5770–5785.

Ohno, N., Miura, N.N., Chiba, N., Adachi, Y., and Yadomae, T. (1995) Comparison of the immunopharmacological activities of triple and single-helical schizophyllan in mice. *Biol Pharm Bull* **18:** 1242–1247.

Park, B.J., Wannemuehler, K.A., Marston, B.J., Govender, N., Pappas, P.G., and Chiller, T.M. (2009) Estimation of the current global burden of cryptococcal meningitis among persons living with HIV/AIDS. *AIDS* **23:** 525–530.

Pirofski, L.A. (2001) Polysaccharides, mimotopes and vaccines for fungal and encapsulated pathogens. *Trends Microbiol* **9:** 445–451.

Radosta, S., Haberer, M., and Vorwerg, W. (2001) Molecular characteristics of amylose and starch in dimethyl sulfoxide. *Biomacromolecules* **2:** 970–978.

Retini, C., Vecchiarelli, A., Monari, C., Tascini, C., Bistoni, F., and Kozel, T.R. (1996) Capsular polysaccharide of *Cryptococcus neoformans* induces proinflammatory cytokine release by human neutrophils. *Infect Immun* **64:** 2897–2903.

Retini, C., Vecchiarelli, A., Monari, C., Bistoni, F., and Kozel, T.R. (1998) Encapsulation of *Cryptococcus neoformans* with glucuronoxylomannan inhibits the antigen-presenting capacity of monocytes. *Infect Immun* **66:** 664–669.

Riccio, R., Kinnel, R.B., Bifulco, G., and Scheuer, P.J. (1996) Kakelokelose, a sulfated mannose polysaccharide with anti-HIV activity from the Pacific tunicate Didemnum molle. *Tetrahedron Lett* **37:** 1979–1982.

Rodrigues, M.L., Nimrichter, L., Oliveira, D.L., Frases, S., Miranda, K., Zaragoza, O., *et al*. (2007) Vesicular polysaccharide export in *Cryptococcus neoformans* is a eukaryotic solution to the problem of fungal trans-cell wall transport. *Eukaryot Cell* **6:** 48–59.

Roger, P., Axelos, M.A.V., and Colonna, P. (2000) SEC,àíMALLS and SANS Studies Applied to Solution Behavior of Linear Œ±-Glucans. *Macromolecules* **33:** 2446–2455.

Rolland-Sabate, A., Colonna, P., Mendez-Montealvo, M.G., and Planchot, V. (2007) Branching features of amylopectins and glycogen determined by asymmetrical flow field flow fractionation coupled with multiangle laser light scattering. *Biomacromolecules* **8:** 2520–2532.

Sasaki, T., and Takasuka, N. (1976) Further study of the structure of lentinan, an anti-tumor polysaccharide from *Lentinus edodes*. *Carbohydr Res* **47:** 99–104.

Stoddart, R.W. (1984) *The Biosynthesis of Polysaccharides*. London: Croom Helm, p. 354.

Tao, Y., and Zhang, L. (2006) Determination of molecular size and shape of hyperbranched polysaccharide in solution. *Biopolymers* **83:** 414–423.

Tao, Y., Zhang, L., and Cheung, P.C. (2006) Physicochemical properties and antitumor activities of water-soluble native and sulfated hyperbranched mushroom polysaccharides. *Carbohydr Res* **341:** 2261–2269.

Tao, Y., Zhang, L., Yan, F., and Wu, X. (2007) Chain conformation of water-insoluble hyperbranched polysaccharide from fungus. *Biomacromolecules* **8:** 2321–2328.

Vaishnav, V.V., Bacon, B.E., O'Neill, M., and Cherniak R. (1998) Structural characterization of the galactoxylomannan of *Cryptococcus neoformans* Cap67. *Carbohydr Res* **306:** 315–330.

Vecchiarelli, A., Retini, C., Pietrella, D., Monari, C., Tascini, C., Beccari, T., and Kozel, T.R. (1995) Downregulation by cryptococcal polysaccharide of tumor necrosis factor alpha and interleukin-1 beta secretion from human monocytes. *Infect Immun* **63:** 2919–2923.

Xiao, G., Miyazato, A., Inden, K., Nakamura, K., Shiratori, K., Nakagawa, K., *et al*. (2008) *Cryptococcus neoformans* inhibits nitric oxide synthesis caused by CpG-oligodeoxynucleotide-stimulated macrophages in a fashion independent of capsular polysaccharides. *Microbiol Immunol* **52:** 171–179.

Yang, L., and Zhang, L.-M. (2009) Chemical structural and chain conformational characterization of some bioactive polysaccharides isolated from natural sources. *Carbohyd Polym* **76:** 349–361.

Yoneda, A., and Doering, T.L. (2006) A eukaryotic capsular polysaccharide is synthesized intracellularly and secreted via exocytosis. *Mol Biol Cell* **17:** 5131–5140.

York, W.S., Darvill, A.G., McNeil, M., Stevenson, T.T., and Albersheim, P. (1985) Isolation and characterization of plant cell walls and cell-wall components. *Methods Enzymol* **118:** 3–40.

Zaragoza, O., Chrisman, C.J., Castelli, M.V., Frases, S., Cuenca-Estrella, M., Rodriguez Tudela, J.L., and Casadevall, A. (2008) Capsule enlargement in *Cryptococcus neoformans* confers resistance to oxidative stress suggesting a mechanism for intracellular survival. *Cell Microbiol* **10:** 2043–2057.

Zaragoza, O., Rodrigues, M.L., Jesus, M.D., Frases, S., Dadachova, E., and Casadevall, A. (2009) The capsule of the fungal pathogen *Cryptococcus neoformans*. *Adv Appl Microbiol* **68:** 133–216.

Zhang, L., Li, X., Xu, X., and Zeng, F. (2005) Correlation between antitumor activity, molecular weight, and conformation of lentinan. *Carbohydrate Res* **340:** 1515–1521.

Zhang, X., Zhang, L., and Xu, X. (2004) Morphologies and conformation transition of lentinan in aqueous NaOH solution. *Biopolymers* **75:** 187–195.

Zhong, F., Yokoyama, W., Wang, Q., and Shoemaker, C.F. (2006) Rice starch, amylopectin, and amylose: molecular weight and solubility in dimethyl sulfoxide-based solvents. *J Agric Food Chem* **54:** 2320–2326.

Supporting information

Additional supporting information may be found in the online version of this article.